Reflective AWG with flattened response

E. Kleijn, M. K. Smit and X. J. M. Leijtens

COBRA Research Institute, Technische Universiteit Eindhoven, Postbus 513,
5600 MB Eindhoven, The Netherlands. Email: e.kleijn@tue.nl

A new principle for flattening AWG responses is demonstrated. The approach works in reflection, where the spectrum of the reflected light shows a box like shape, with only a small passband ripple. The method is in principle lossless. The main part of the device is formed by a general multimode interference reflector. This MIR works as a retro-reflector that not only preserves the field shape, but also the position of the field. A pure propagation direction reversal is obtained in this way. The theory behind the principle is explained, and we present simulation results and initial measurement results.

Introduction

Various methods for flattening the response of Arrayed Waveguide Gratings (AWGs) have been proposed. The most prominent are using multimode output waveguide [1], parabolic input tapers [2], dual focal point arrays [3], and synchronized designs [4]. The first three methods increase the insertion loss of the AWG. The last method is in principle lossless, but is quite complex to realize. We propose to use a special multimode interference reflector (MIR) [5], which is inserted in the output free propagation region (FPR) of an AWG. Light within the MIR aperture is reflected back while light outside the aperture is not. This leads to a flat reflection band. When using a platform suitable for active-passive integration, the reflector itself can be made active. This would enable the reflected light to be modulated by a data signal. An application for such a device would be as an optical network unit (ONU) in a passive optical network [6]. Such an ONU should be wavelength-independent and cost-competitive [6]. The device presented here could fulfill both requirements.

Theory

MIRs are on-chip reflectors that are based on MMIs [5]. Such a reflector consists of two 45° mirrors and a multimode section, as shown in Fig. 1a. By choosing the length of the reflector equal to $L_{\mathrm{MIR}} = 1.5 \cdot L_{\pi}$, a so called general interference 1-port reflector is obtained [5]. Here L_{π} is the familiar beat length from MMI theory, between the fundamental and first order mode in the multimode section of the device [7]. Though this device is markedly longer than a 1-port reflector based on symmetric interference, it offers some interesting properties. The most significant of which is its ability to reflect an arbitrary shaped input field. What this means is that the location of the input waveguide is not restricted to a single position. In other words, the value of x' in Fig. 1a can be chosen freely along the MIR input aperture.

The field at the input of the MIR does not have to be guided there by a waveguide. It can also be imaged through a free propagation region, like the one found in an AWG. Due to the dispersive properties of AWGs, the spot at the output side moves as a function of

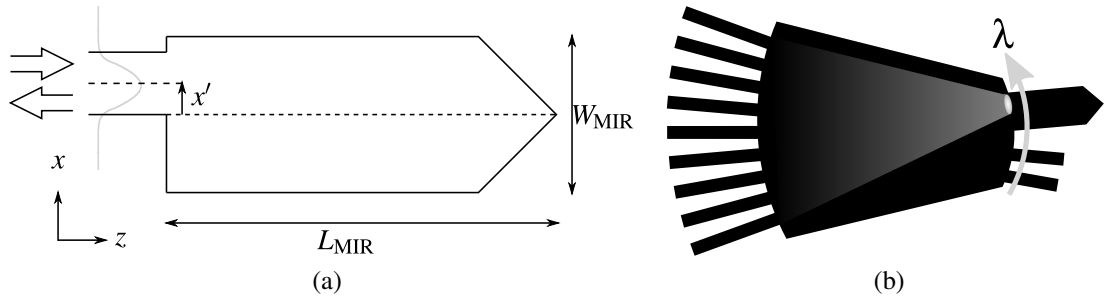

Fig. 1: (a) Generic MIR layout. An input field is launched from position $x = x'$, and is imaged back to the same position. This accomplishes a pure propagation reversal which has only a small dependence on the position x'. (b) Schematic representation of the output FPR. The array waveguides are shown on the left, and the regular output waveguides on the right. Light is focused onto a position that depends on the wavelength λ of the input signal, as indicated by the arrow.

wavelength. This is shown schematically in Fig. 1b. The spot will be reflected back as long as it is within the aperture of the MIR.

Simulation

The fundamental mode of a 2 µm wide waveguide is launched at the input side of an AWG. The coupling through the AWG to the modes of order ν in a multimode waveguide was calculated using an analytical model [8]. This model calculates the coupling T_ν by taking the overlap between the AWG output field and each of the modes. The multiple modes are then propagated by multiplying them by a phase factor $\exp(-j[2\beta_\nu L_{\mathrm{MIR}} + \pi\nu])$, where β_ν is the mode dependent propagation constant. The factor $\pi\nu$ causes all odd modes to be flipped, which models the effect of the 45° mirrors. Finally, all modes are propagated through the same AWG again, and the overlap with the input mode is taken. The total reflection is thus modeled as

$$R = \sum_\nu T_\nu \exp(-j[2\beta_\nu L_{\mathrm{MIR}} + \pi\nu]) T_\nu \tag{1}$$

Fig. 2 shows the simulated reflection using (1) for an AWG designed for the COBRA InP layer stack. An 8 µm wide MIR is connected to the output FPR. The central wavelength of the AWG is 1550 nm, the dispersion is 50 GHz/µm, and the free spectral range is 1800 GHz. The input waveguide is 2 µm wide. The simulation results clearly show a flattened response. A difference in passband ripple can be seen between TE and TM. This is caused by the birefringence of the layer stack, and a resulting different optimal wavelength for TM. The passband is slightly slanted with the short wavelength side being 0.6 dB lower than the long wavelength side, because the MIR is connected to the FPR with an angle of $-4.0°$. The 3 dB bandwidth is 2.59 nm (332 GHz). This is much larger than the non-flattened bandwidth of 0.72 nm (90 GHz).

Measurement

After fabrication at NanoLab@TU/e the chips were anti-reflection coated and characterized. Light from a tunable laser source was coupled into the chip by using a microscope

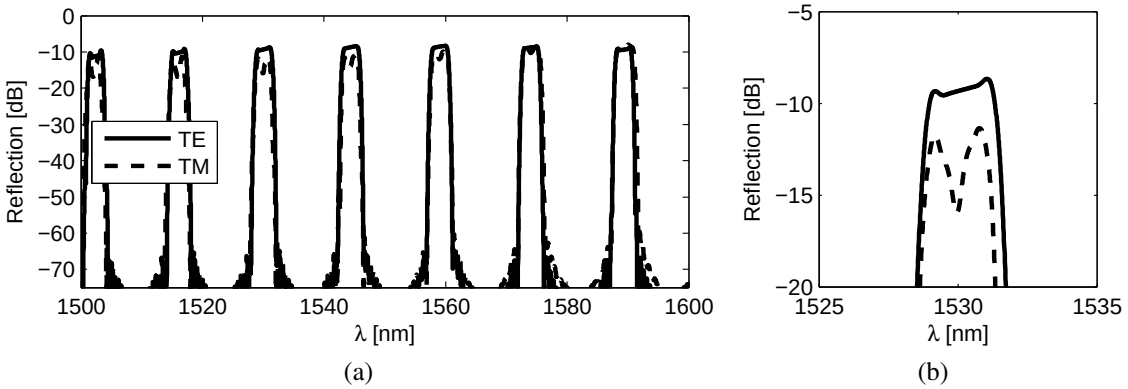

Fig. 2: Simulation of the reflective bandpass filter response for TE and TM. (a) Three FSRs of the flattened AWG response. (b) Close-up of the passband closest to the central wavelength. The ripple in the TM polarized passband signal is due to a different optimal wavelength for this polarization.

objective, which focused a collimated beam from a fiber launch stage onto the chip facet. A circulator allowed the back reflected signal to be recorded. A polarizing beam splitter was inserted in the collimated beam, and set to pass TE polarized light.
Figure 3 shows the measured back-reflected signal. The residual reflection of the coating, estimated to be between -20 dB and -30 dB, together with the strong reflection of the MIR, gave rise to significant fringes within the passband. Outside the passband the fringes are caused by interference between the residual facet reflection and the crosstalk of the circulator. The difference in reflectivity in-band and out-of-band was measured to be 14 dB. By improving the anti-reflection coating and the circulator isolation, this difference can be increased to 24 dB, which is the measured AWG crosstalk level. There is a strong dip in the middle of the passband. At this point it is unclear what causes this, but it is known that a deviation of the design width of the MIR causes ripples in the passband. Another possibility is a distortion of the phase front along the aperture of the MIR because of a slight oblique incidence. Also polarization rotation effects inside the AWG could play a role. When we ignore the dip, the 3 dB passband width is 2.6 nm. This is extremely close to the design width of 2.59 nm.

Conclusion

A new method of flattening the passband of an AWG was introduced, which works in reflection mode. Devices using this new principle were fabricated and characterized. Measurements showed that a strong dip is present in the passband. The 3 dB passband width is 2.6 nm in the measured device, which is extremely close to the design width of 2.59 nm. More measurements and modeling are necessary to understand the cause of the dip. If this effect can be mitigated, the presented device could be used, for example, as a reflective optical network unit in passive optical networks.

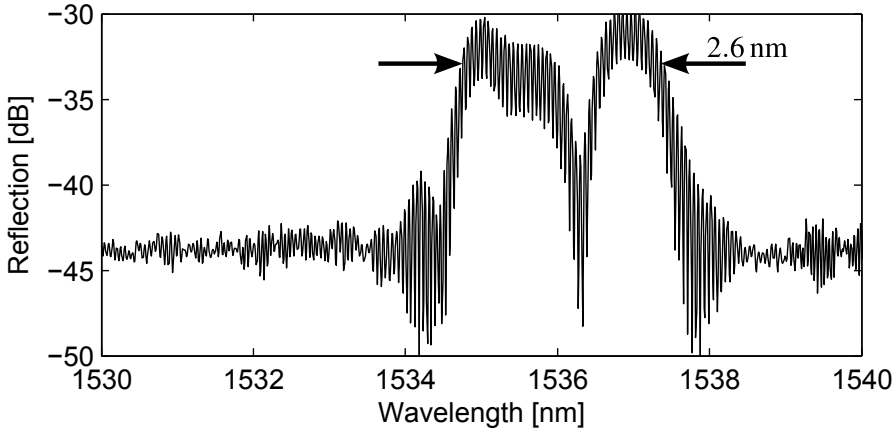

Fig. 3: Measured response of passband flattened AWG. The passband shows an unexpected dip in the center. Ignoring this dip, the 3 dB passband width is 2.6 nm. The reflection level was normalized to the maximum in the passband.

Acknowledgments

The research leading to these results has received funding from the European Community's Seventh Framework Programme FP7/2007-2013 under grant agreement ICT 257210 PARADIGM. The authors wish to thank D. D'Agostino for coating the chips with a silicon nitride anti-reflection coating.

References

[1] M.R. Amersfoort, C.R. de Boer, F.P.G.M. van Ham, M.K. Smit, P. Demeester, J.J.G.M. van der Tol, and A. Kuntze. Phased-array wavelength demultiplexer with flattened wavelength response. *Electron. Lett.*, 30(4):300–302, February 1994.

[2] K. Okamoto and H. Yamada. Flat spectral response arrayed waveguide grating multiplexer with parabolic waveguide horns. *Electron. Lett.*, 32(18):1661–1662, August 1996.

[3] D. Trouchet, A. Beguin, H. Boek, C. Prel, C. Lerminiaux, and R.O. Maschmeyer. Passband flattening of phasar wdm using input and output star couplers designed with two focal points. In *Optical Fiber Communication. OFC 97., Conference on*, pages 302–303, 1997.

[4] C.R. Doerr, L.W. Stulz, and R. Pafchek. Compact and low-loss integrated box-like passband multiplexer. *IEEE Photon. Technol. Lett.*, 15(7):918–920, July 2003.

[5] Emil Kleijn, Meint Smit, and Xaveer Leijtens. Multimode interference reflectors: a new class of components for photonic integrated circuits. *J. Lightwave Technol.*, 2013. doi:10.1364/AO.51.000789.

[6] Wooram Lee, Mahn Yong Park, Seung Hyun Cho, Jihyun Lee, Chulyoung Kim, Geon Jeong, and Byoung Whi Kim. Bidirectional WDM-PON based on gain saturated reflective semiconductor optical amplifiers. *IEEE Photon. Technol. Lett.*, 17(11):2460–2462, November 2005.

[7] L.B. Soldano and E.C.M. Pennings. Optical multi-mode interference devices based on self-imaging: Principles and applications. *J. Lightwave Technol.*, 13(4):615–627, April 1995.

[8] Emil Kleijn, Meint K. Smit, and Xaveer J.M. Leijtens. New analytical arrayed waveguide grating model. *J. Lightwave Technol.*, 2013.